UMTA-MA-06-0153-85-7
DOT-TSC-UMTA-86-2

U.S. Department
of Transportation
**Urban Mass
Transportation
Administration**

Inductive Interference in Rapid Transit Signaling Systems
Volume I: Theory and Background

F. Ross Holmstrom

Transportation Systems Center
Cambridge, MA 02142

May 1986
Reprint
May 1987
Final Report

UMTA Technical Assistance Program

NOTICE

This document is disseminated under the sponsorship of the Department of Transportation in the interest of information exchange. The United States Government assumes no liability for its contents or use thereof.

NOTICE

The United States Government does not endorse products of manufacturers. Trade of manufacturers' names appear herein solely because they are considered essential to the object of this report.

Technical Report Documentation Page

1. Report No.	2 Government Accession No.	3. Recipient's Catalog No.
UMTA-MA-06-0153-85-7		

4. Title and Subtitle	5. Report Date	6. Performing Organization Code
INDUCTIVE INTERFERENCE IN RAPID TRANSIT SIGNALING SYSTEMS, VOLUME I: THEORY AND BACKGROUND	May 1986 Reprint May 1987	DTS-77

7. Author(s)	8. Performing Organization Report No.
F. Ross Holmstrom	DOT-TSC-UMTA-86-2

9. Performing Organization Name and Address	10. Work Unit No. (TRAIS)	11. Contract or Grant No.
U.S. Department of Transportation Research and Special Programs Administration Transportation Systems Center Cambridge, MA 02142	UM676/U6601	

12. Sponsoring Agency Name and Address	13. Type of Report and Period Covered	14. Sponsoring Agency Code
U.S. Department of Transportation Urban Mass Transportation Administration Office of Technical Assistance Washington, DC 20590	Final Report April 1979-February 1986	URT-12

15. Supplementary Notes

16. Abstract

This report analyzes the problem of inductive interference with audio-frequency signaling caused by chopper-controlled propulsion systems on rapid transit vehicles. After discussing audio-frequency track circuits, the report examines chopper interference generation as well as methods for observing and recording interference signals.

The report develops a physical model for calculating levels of inductive interference, gives selected results of field observations, and discusses methods for alleviating the problem, such as improved track signal detection, frequency-domain coding, and new chopper components that generate less stray flux.

17. Key Words	18. Distribution Statement
Automatic Train Control Systems Chopper-Controlled Propulsion Systems Audio-Frequency Signaling Systems Inductive Interference	DOCUMENT IS AVAILABLE TO THE PUBLIC THROUGH THE NATIONAL TECHNICAL INFORMATION SERVICE, SPRINGFIELD VIRGINIA 22161

19. Security Classif. (of this report)	20 Security Classif (of this page)	21. No. of Pages	22. Price
UNCLASSIFIED	UNCLASSIFIED	44	

PREFACE

Chopper-controlled propulsion systems on subway cars can cause inductive interference with audio-frequency signaling systems, when time-varying magnetic flux lines emanating from chopper systems on vehicles pass through the rail-axle loops under the cars. When a vehicle passes over points at which track circuit receivers are connected to the rails, inductively generated interfering signals can cause track circuits to malfunction. Observation of such interference led directly to the establishment of the Rail Transit EMI Technical Working Group, under the sponsorship of UMTA/DOT.

Development of the theory of inductive interference presented in this report was furthered by discussions at meetings of the Rail Transit EMI Technical Working Group (EMI/TWG) at the DOT Transportation Systems Center in 1979, led by EMI/TWG's founding chairman,Louis Frasco. Many people participated in these discussions. The author extends sincere thanks to all members of that body for lending their knowledge and insights; especially to Messrs. Hoelscher, Matty, Nene, Phelps, Rhoton, Stark, Truman, and Vaughn, whose names appear in the References. The propulsion and signal manufacturers - General Electric, Westinghouse Electric, Garrett Corporation, Union Switch & Signal, and General Railway Signal - have been most cooperative in these activities. A special note of thanks is due to the personnel of BART, CTA, MARTA, MBTA, and NYCTA for their invaluable assistance in gathering field data. A final note of thanks for encouragement and guidance in this effort goes to the sponsor of the UMTA program in rail transit EMI/EMC - Ronald Kangas, Chief of the Design Division, UMTA Office of Systems Engineering.

Much of the material in this report comes from a University of Lowell Research Foundation report by F. Ross Holmstrom, "Chopper Induced Interference in Audio-Frequency Automatic Train Control Systems," final report on DOT Contract No. DOT-TSC-1697, March 1980. This report originally appeared in essentially the same form as a paper by F. Ross Holmstrom, Louis A. Frasco, Robert Gagnon, and Eugene T. Leonard, "Inductive Interference in Audio-Frequency Rapid Transit Signaling Systems Due to Chopper Propulsion Control," presented at the IEEE Industrial Applications Society Annual Meeting, Philadelphia, 5-9 Oct. 1981. The contributions of the original co-authors were invaluable to this report, as they were to the prior paper.

METRIC CONVERSION FACTORS

Approximate Conversions to Metric Measures

Symbol	When You Know	Multiply by	To Find	Symbol
		LENGTH		
in	inches	*2.5	centimeters	cm
ft	feet	30	centimeters	cm
yd	yards	0.9	meters	m
mi	miles	1.6	kilometers	km
		AREA		
in^2	square inches	6.5	square centimeters	cm^2
ft^2	square feet	0.09	square meters	m^2
yd^2	square yards	0.8	square meters	m^2
mi^2	square miles	2.6	square kilometers	km^2
	acres	0.4	hectares	ha
		MASS (weight)		
oz	ounces	28	grams	g
lb	pounds	0.45	kilograms	kg
	short tons (2000 lb)	0.9	tonnes	t
		VOLUME		
tsp	teaspoons	5	milliliters	ml
Tbsp	tablespoons	15	milliliters	ml
fl oz	fluid ounces	30	milliliters	ml
c	cups	0.24	liters	l
pt	pints	0.47	liters	l
qt	quarts	0.96	liters	l
gal	gallons	3.8	liters	l
ft^3	cubic feet	0.03	cubic meters	m^3
yd^3	cubic yards	0.76	cubic meters	m^3
		TEMPERATURE (exact)		
°F	Fahrenheit temperature	5/9 (after subtracting 32)	Celsius temperature	°C

*1 in. = 2.54 cm (exactly). For other exact conversions and more detail tables see NBS Misc. Publ. 286, Units of Weight and Measures. Price $2.25 SD Catalog No. C13 10 286.

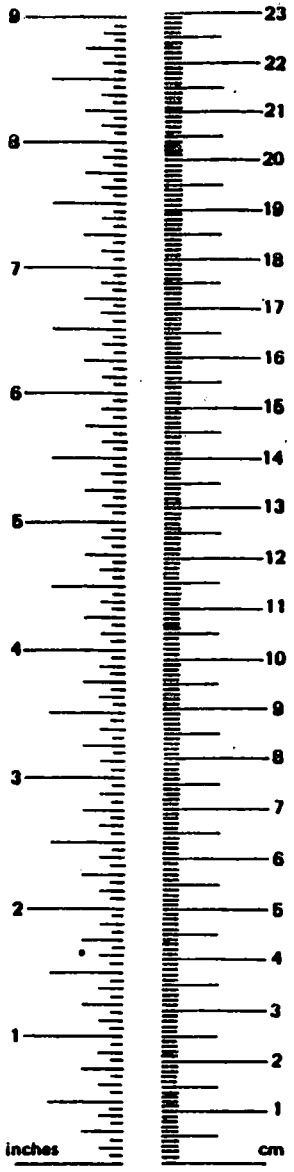

Approximate Conversions from Metric Measures

Symbol	When You Know	Multiply by	To Find	Symbol
		LENGTH		
mm	millimeters	0.04	inches	in
cm	centimeters	0.4	inches	in
m	meters	3.3	feet	ft
m	meters	1.1	yards	yd
km	kilometers	0.6	miles	mi
		AREA		
cm^2	square centimeters	0.16	square inches	in^2
m^2	square meters	1.2	square yards	yd^2
km^2	square kilometers	0.4	square miles	mi^2
ha	hectares (10,000 m^2)	2.5	acres	
		MASS (weight)		
g	grams	0.035	ounces	oz
kg	kilograms	2.2	pounds	lb
t	tonnes (1000 kg)	1.1	short tons	
		VOLUME		
ml	milliliters	0.03	fluid ounces	fl oz
l	liters	2.1	pints	pt
l	liters	1.06	quarts	qt
l	liters	0.26	gallons	gal
m^3	cubic meters	36	cubic feet	ft^3
m^3	cubic meters	1.3	cubic yards	yd^3
		TEMPERATURE (exact)		
°C	Celsius temperature	9/5 (then add 32)	Fahrenheit temperature	°F

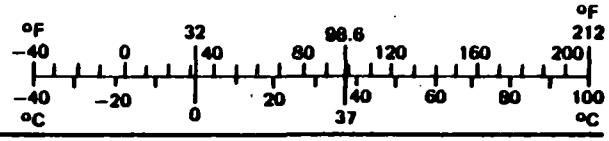

TABLE OF CONTENTS

		Page
1.	INTRODUCTION	1
2.	AUDIO-FREQUENCY TRACK CIRCUITS	3
3.	CHOPPER INTERFERENCE GENERATION: THE CHOPPER CIRCUIT	11
4.	CHOPPER INTERFERENCE GENERATION: THE RAIL CIRCUIT	19
5.	OBSERVATION AND RECORDING OF CHOPPER INTERFERENCE SIGNALS	22
6.	DIAGNOSIS AND REDUCTION OF CHOPPER INTERFERENCE	29
7.	CONCLUSION	32
REFERENCES		33

FIGURES

Page

1. An audio-frequency automatic train control system 4
2. Wayside equipment for audio-frequency ATC systems 5
3. $Z_{IB}(f)$ for a GRS impedance bond 7
4. $Z_{IB}(f)$ for a US&S impedance bond 8
5. Configuration of car and signaling equipment leading to inductive chopper interference 12
6. A chopper circuit showing wiring for propulsion mode 14
7. Idealized waveforms of magnetic flux from motor smoothing reactor and commutation reactor, and corresponding emf's . . 15
8. Amplitudes of Fourier series components of $\dot{\Phi}_M$ and $\dot{\Phi}_C$, for the case $f_c = 10\ f_m$, $\delta = 0.5$ 17
9. Circuit for source of inductive interference and its Thevenin equivalent 20
10. Instrumentation for observing and recording inductive interference 23
11. Waveforms of open-circuit rail-to-rail voltage during passage of a car 25
12. FFT spectral plots of rail-to-rail inductive interference voltage 27
13. RMS amplitude of a single interference spectral line vs. time as train passes 28

EXECUTIVE SUMMARY

Two electronic techniques simultaneously are experiencing greater use in rail transit operation in the U.S. The first is thyristor chopper control of rapid transit propulsion. The second is use of audio-frequency track circuits for automatic train control and signaling. Chopper propulsion control offers greater energy efficiency due to elimination of series starting resistors, and due to its compatibility with regenerative braking. Audio-frequency track circuits are used easily with continuous cab signaling, which leads to greater operational efficiency and flexibility.

However, the use of chopper-controlled propulsion systems on rapid transit vehicles can cause inductive interference with audio-frequency signaling systems. Inductive interference is caused by the time-varying magnetic flux lines, emanating from propulsion equipment on the vehicle, passing through the rail-axle loop under the vehicle. It is evidenced by observation of abnormally high levels of rail-to-rail voltage observed at locations under the vehicle. The passage of a vehicle over a fixed point induces a transient interference voltage from rail to rail that can have significant harmonic content throughout the audio-frequency spectrum. The induced voltage can be coupled into audio-frequency track circuit receivers, and can disrupt their normal operation.

In the future, U.S. rapid transit vehicles will be powered by ac traction motors, with solid-state inverters and power controllers used to provide the power of variable frequency, current, and voltage required by the motors. These systems will offer further operating economies, but will share with dc chopper systems the potential to cause inductive interference with audio-frequency signaling systems.

A physical model for calculating levels of inductive interference is developed in this report. Selected results of field observations are given, and methods for alleviating the problem are discussed.

1. INTRODUCTION

Two electronic techniques simultaneously are experiencing greater use in rapid transit operation in the U.S. The first is thyristor chopper control of rail car propulsion [Ref. 1]. The second is use of audio-frequency (AF) track circuits for automatic train control and signaling [Ref. 2]. Chopper propulsion control offers greater energy efficiency due to elimination of series starting resistors, and due to its compatibility with regenerative braking. AF track circuits are used easily with continuous cab signaling, which leads to greater operational efficiency and flexibility. These track circuits also can be employed on track made up of continuously welded rail, leading to smoother ride and lower track maintenance. Unfortunately, interference problems can occur when these techniques are used simultaneously.

This report describes the mechanism of inductive interference to AF signaling systems used in rail transit operations, caused by rail transit vehicles with chopper propulsion control. Choppers are switching circuits composed of high-power semiconductor devices, inductors, and capacitors. In operation, choppers control propulsion power by pulsing the dc voltage to the dc traction motors on and off at a rate of a few hundred Hertz. Power is controlled by varying the pulse rate, the pulse width, or both. Due to the pulsed nature of voltage and current waveforms, harmonics of voltages and currents in the chopper system are produced that extend in frequency through the AF range, and can affect adversely the performance of AF signaling systems. Such interference has been observed in actual transit operation in the U.S.

In the future, rapid transit cars powered by ac induction motors will be used in the U.S., as they currently are elsewhere. These "ac drive" propulsion systems employ solid-state switching circuits to transform dc third-rail power into the three-phase ac power of variable voltage, current, and frequency, that powers the motors. The approaches outlined in this report for dealing with inductive interference from dc chopper propulsion control systems serve as a good starting point for analyzing inductive interference of the new ac drive systems. However, this report deals only with dc chopper systems, since these were the subject of actual field investigation in this program.

Inductive interference is caused by time-varying magnetic flux lines, emanating from propulsion equipment on the vehicle, passing through the rail-axle loop under the vehicle. It is evidenced by the observation of abnormally high levels of AF rail-to-rail voltage observed at locations under the vehicle. The passage of a vehicle over a fixed location induces a transient interference voltage from rail to rail which can have measurable harmonic content throughout the AF spectrum. The induced voltages are coupled into AF track circuit apparatus, and can disrupt the normal operation of such equipment. A physical model for calculating interference levels observed is developed in this report, and results of field observations are given.

To guard against conductive interference, caused by AF currents in the third rail, chopper manufacturers take special precaution in design of traction power line filters, to reduce chopper harmonic components of current to acceptable levels. AF currents flowing in the running rails, which serve as the dc propulsion current return path, always have some measure of imbalance, leading to a differential or circulating component. It was well known that the resulting conductive interference could affect operation of AF track circuits [Ref's 3 - 6]. The problem of inductive interference was less well anticipated.

A program to solve the problem of inductive interference was undertaken, and included the cooperative efforts of signal and propulsion equipment manufacturers, affected rail transit systems, and the Transportation Systems Center of the U.S. Dept. of Transportation (DOT/TSC) under the sponsorship of the UMTA Office of Rail Technology [Ref's 7 - 9]. One product of this program is a set of suggested test procedures for assuring compatibility of propulsion and signaling systems [Ref. 10].

2. AUDIO-FREQUENCY TRACK CIRCUITS

Historically, the AF automatic train control (ATC) systems for which chopper interference was reported most widely are of the type manufactured by General Railway Signal Co. (GRS) [Ref. 11], and the Union Switch and Signal Division of American Standard, Inc. (US&S) [Ref's 12, 13]. Figure 1 shows a schematic diagram of this type of system. The discussion that follows is meant to describe the most general operating principles and characteristics of a few types of AF track circuits. To show examples of analysis and data gathering techniques, data are presented on a very limited number of specific systems; however, these data are not specifically characteristic of other systems, even those built by the same manufacturers. Therefore, they should not be used as standards or for setting specification limits.

For the ATC system to detect a train in a given block, an amplitude-modulated AF signal of specific carrier frequency is transmitted from one AF impedance bond (IB) to the next, down the transmission line formed by the rails. The IB, the transmission line feeding the IB, and other components in the wayside bungalow comprise a tuned resonant circuit that passes signals at the desired train detection frequency. When a train enters a given block, reception of the train detection signal at the receiver end of the block ceases, causing that block's track relay to drop. Dropping of the track relay actuates transmission of a train speed command signal at another audio frequency, from the transmitting IB down the rails to the train.

Figure 2 describes the operation of the ATC track receiver into which both true and interfering signals are coupled. (This figure does not represent specific circuitry.) The IB is a voltage step-up transformer located at the tracks, that is used for impedance matching between the low track impedance (a few ohms at AF) and the high impedance levels of the receiver and transmitter. The IB is followed by a tuned multi-resonant filter. The filter is comprised of ganged shunt-resonant circuits - one circuit for each frequency used at a particular location. The impedance of the filter has peaks at each of the frequencies at which a particular IB transmits or receives signals - typically three or four in number: The carrier frequencies for train detection in adjacent blocks, f_{XMT} and f_{RCV}, and one or two carrier frequencies for transmitting coded ATC signals to the train f_{CAB}.

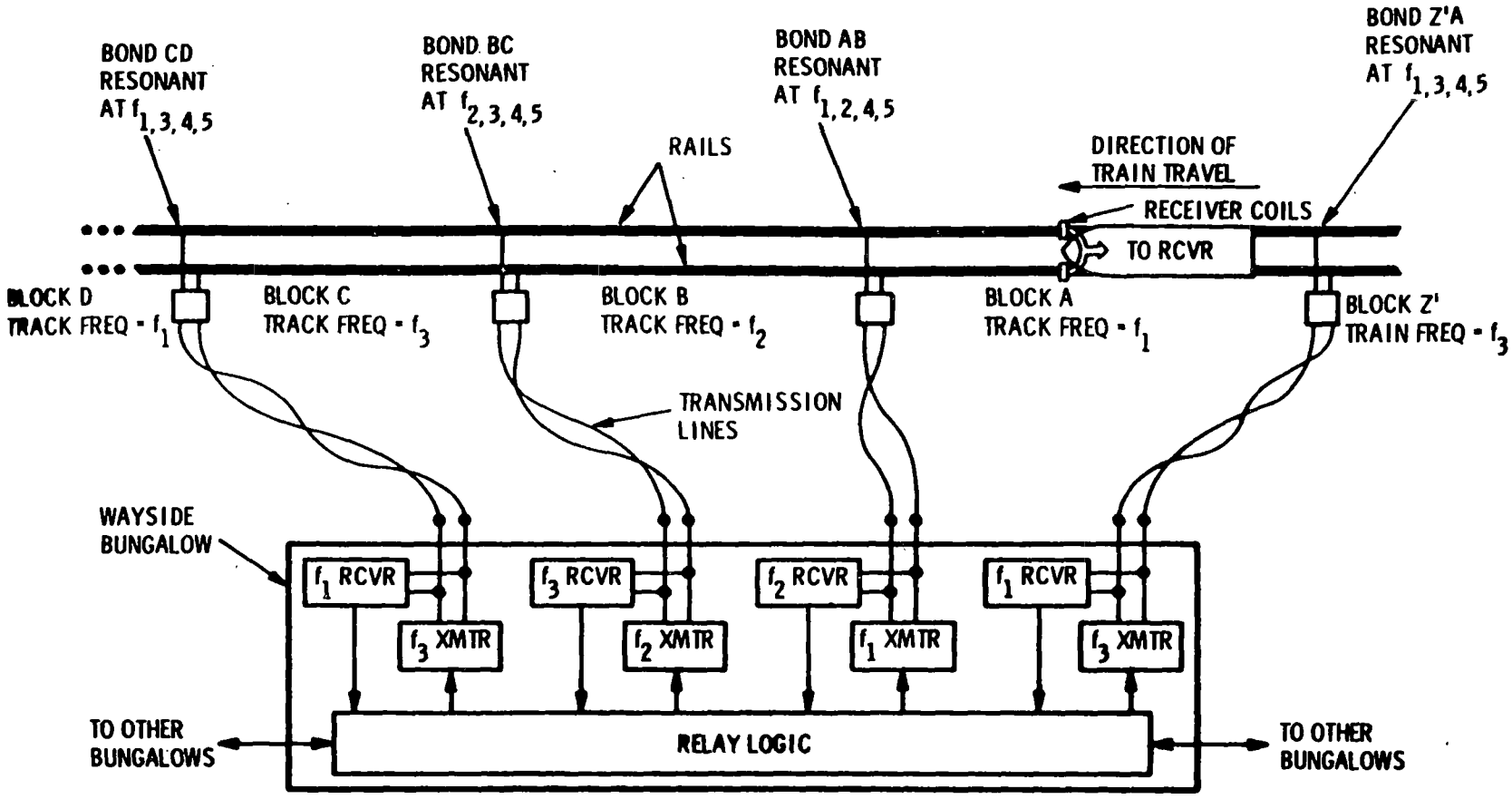

FIGURE 1. An audio-frequency automatic train control system.

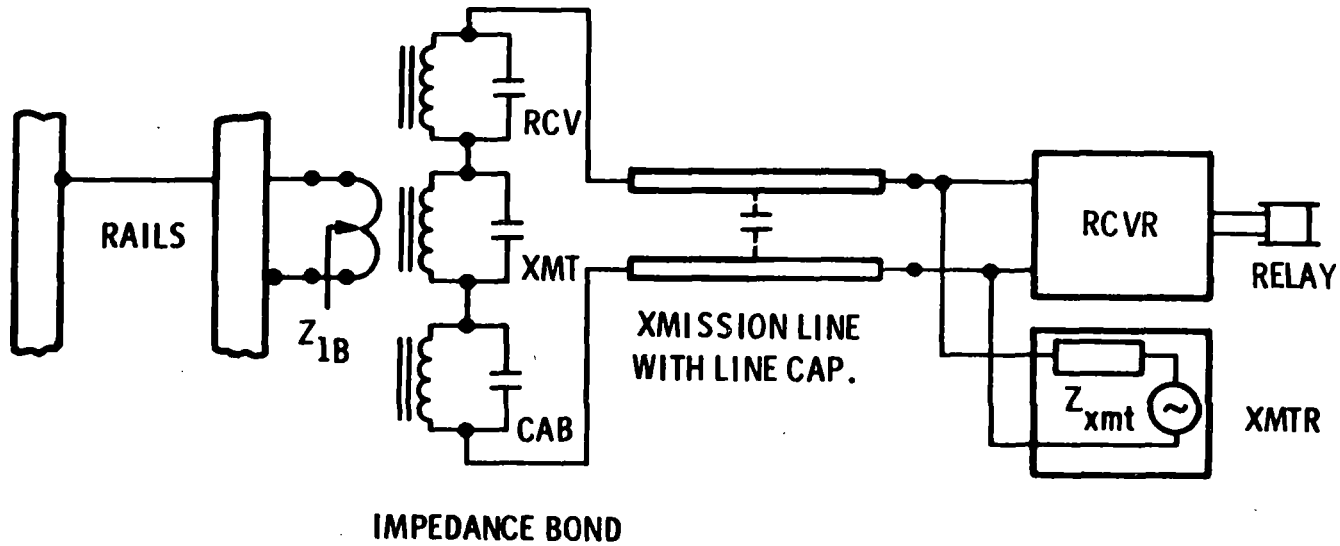

a. THE CIRCUIT

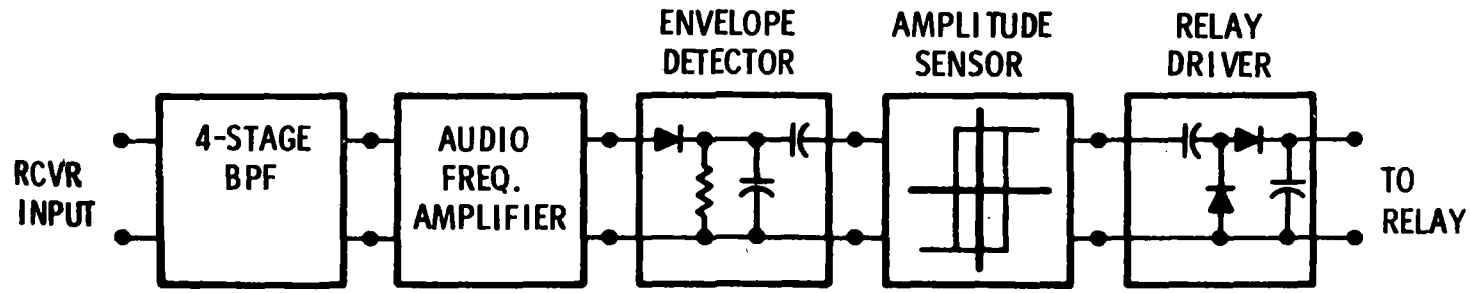

b. THE RECEIVER

FIGURE 2. Wayside equipment for audio-frequency ATC systems.

These frequencies lie between 990 Hz and 7 kHz in GRS and US&S systems. The impedance characteristics of the circuits are affected by the the transmitter output impedance Z_{xmt}, and receiver input impedance. Typical IB input impedances Z_{IB}, seen looking into the track terminals of the IB are shown in Figures 3 and 4, for representative examples of US&S and GRS equipment. Z_{IB} peaks at each resonant frequency of the coupling filter, at frequencies near each carrier frequency of signals transmitted by the IB. A variety of operational and engineering factors affects the choices the manufacturer makes for peak values of Z_{IB}, and these change from one application to another.

In normal operation, the receiver accepts a signal at frequency f_{RCV}, which is at the center of the passband of a 4-stage band-pass receiver filter. The signal is 100% amplitude-modulated at a variable code rate. The code rate specifies the train's allowed speed. Bursts of cab and track signal are interleaved, thus limiting required peak signal levels that must be generated by the transmitter. Since the track receiver does not make use of code rate information, it is designed to operate with any code rate within the range used, typically 1 to 20 Hz. The received filtered signal is amplified and envelope-detected to produce an ac signal whose frequency is the code rate. The amplitude of this signal is then sensed, and if it is sufficient, the track relay is picked up.

The receiver filter's -3db bandwidth is typically appx. 8% of the center frequency in existing systems. Narrower filters can be employed. The minimum -3db bandwidth is twice the maximum code rate - the bandwidth required for passage of the first-order modulation sidebands of the amplitude-modulated track signal.

Because of its design and operation, the receiver will respond to a broad variety of interfering signals whose frequencies lie within or sufficiently near the passband of the receiver filter, have sufficient amplitude, and are of a pulsating nature. In some ATC systems, notably the GRS system installed on the Braintree-to-Andrew portion of the MBTA Red Line in Boston, and older parts of the GRS system installed on the CTA rapid transit lines, two or three separate pulses of AF signal must be received for the track relay to pick up.

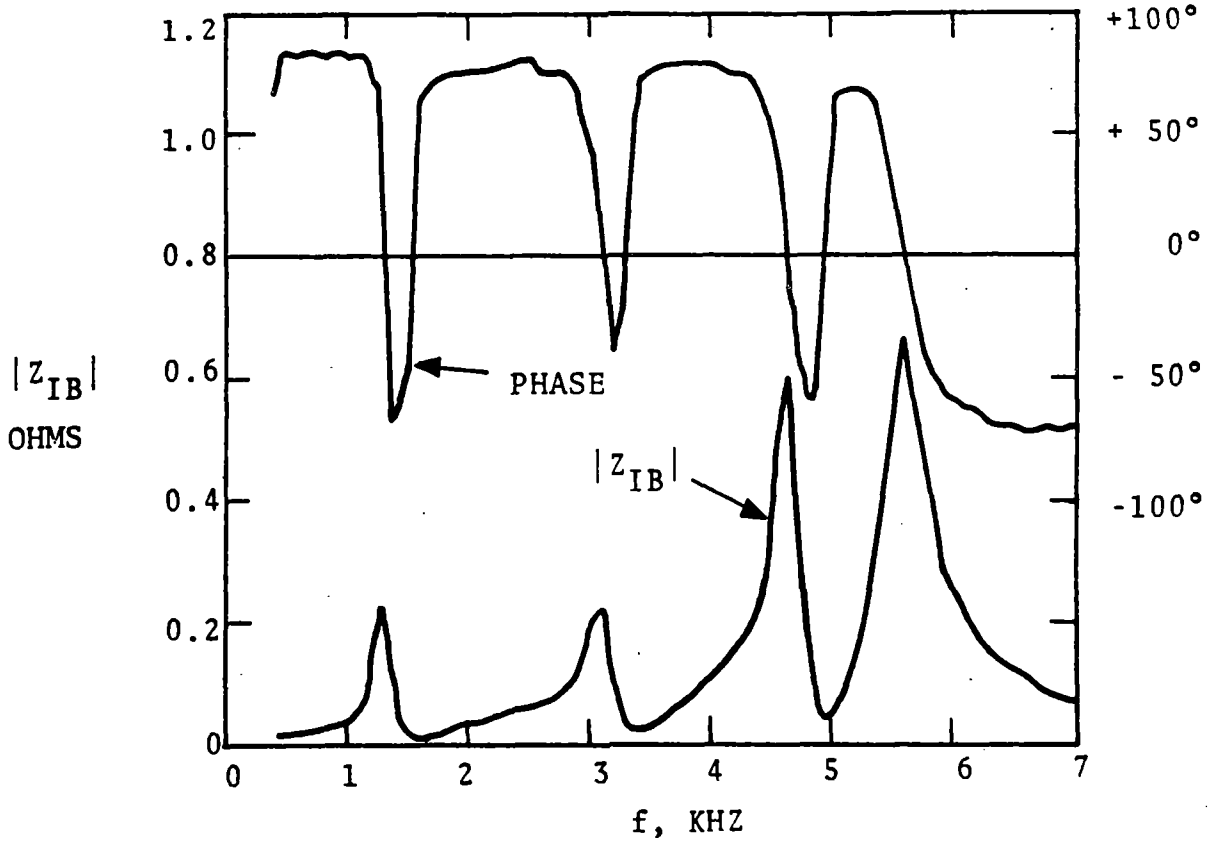

FIGURE 3. $Z_{IB}(f)$ for a GRS impedance bond.

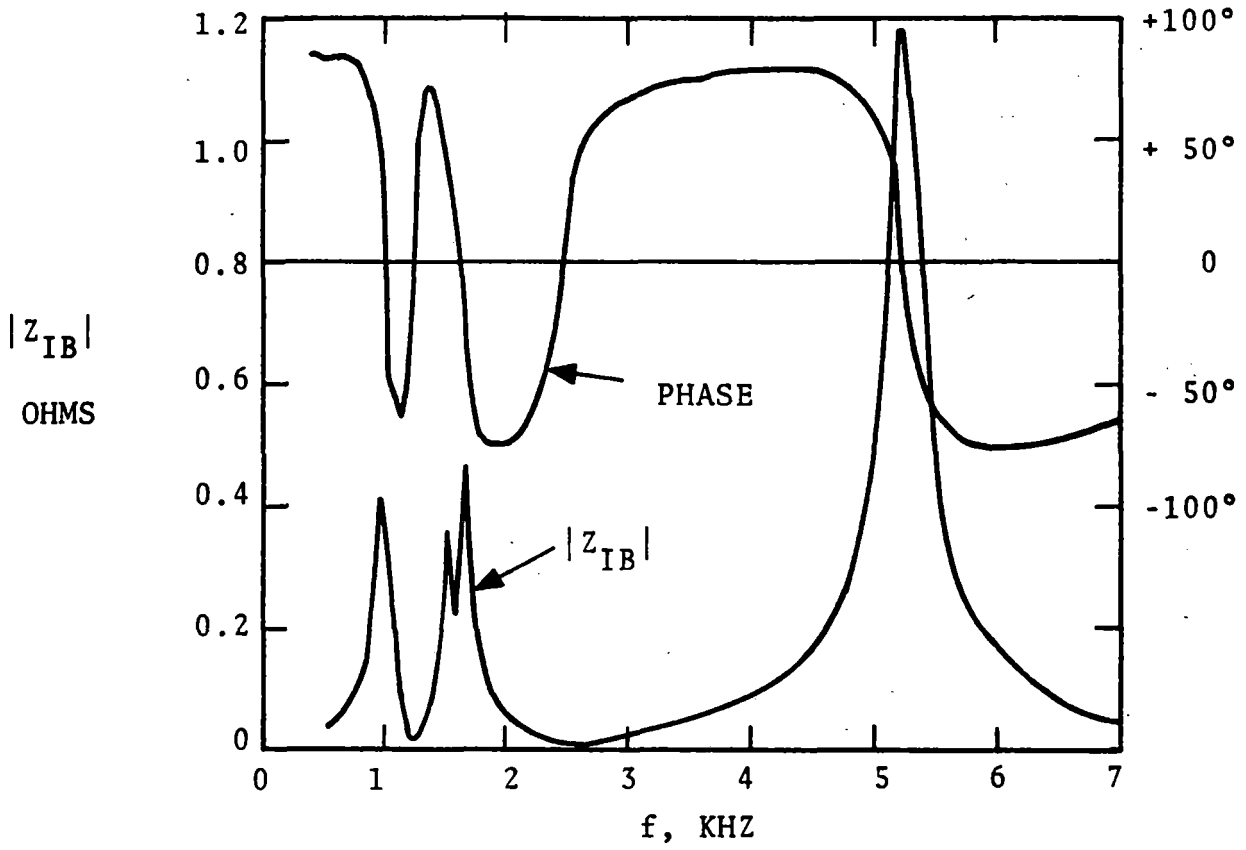

FIGURE 4. $Z_{IB}(f)$ for a US&S impedance bond.

In more recent systems designed for minimum-headway quick-response operation, a single leading edge of a burst will cause the track relay to pick up momentarily. However, the relay will drop again unless the signal continues in a pulsating manner.

Momentary lifting of the track relay can give a momentary false clear indication, and can lead to interruption of transmission of a speed command signal to the train, which in turn can lead to momentary loss of propulsion, or initiation of braking. The specific consequences depend on the timing and circuit characteristics of the system involved. If receiver filter characteristics and circuit characteristics of the IB are known, susceptibility of a signaling system to chopper interference at any frequency can be assessed.

Table 1 lists typical threshold signal levels within the passband of the receiver filter, required to pick up the track relay, for US&S and GRS systems. These figures should be regarded only as order-of-magnitude references, since higher or lower levels would be used for specific applications.

The US&S data were obtained by making measurements on US&S equipment supplied for test operation on the MBTA Haymarket-North line in Boston. US&S receivers are designed to have greater sensitivity at higher frequencies, since attenuation in the rails is greater at higher frequencies, and received signal levels consequently tend to be lower.

The GRS data were provided by GRS. They are based on calculation of theoretical maximum receiver sensitivity assuming that all component tolerances are taken to their limits in the direction that increases sensitivity, and that the receiver sensitivity adjustment is set for maximum sensitivity. These data were verified by measurements made on GRS equipment at the MBTA. In practice, a GRS receiver typically is adjusted so that the threshold level is appx. 0.075 vrms (-22.5 dbv) at the track terminals of the IB.

TABLE 1

Threshold Signal Levels at Track Terminals of Impedance Bond Required to Pick Up Track Relay

US&S

(Measured for each rcvr frequency at 10 Hz code rate, 50% duty cycle, 1:40 IB turns ratio.)

f_{rcv} Hz	V_{IB} during on-portion of burst volts rms	dbv*
1590	.054	-25.4
2670	.056	-25
2870	.035	-29
5190	.020	-34

GRS

(Calculated assuming 1:25 IB turns ratio, 6 db rcvr filter attenuation, and assuming all tolerances are taken in direction that increases sensitivity.)

f_{rcv} Hz	V_{IB} during on-portion of burst volts rms	dbv*
All freq's	.017	-35

* $V_{dbv} = 20 \log_{10}(V_{rms})$

3. CHOPPER INTERFERENCE GENERATION: THE CHOPPER CIRCUIT

The earliest U.S. observation of chopper interference with AF track circuits was made in 1978 in Chicago during CTA testing of CTA 2400 Series cars manufactured by Boeing-Vertol and equipped with General Electric (GE) chopper-controlled dc propulsion systems. Similar observations were made in Atlanta during pre-revenue operation of MARTA cars manufactured by Franco-Belge and powered by Garrett chopper systems [Ref. 14]. Subsequent observations of qualitatively similar chopper interference signals were made of experimental NYCTA R-46 cars manufactured by Pullman and powered by GE choppers [Ref. 15], and of BART cars manufactured by Rohr and powered by Westinghouse Electric choppers.*

It was observed at CTA and MARTA that interference signals had characteristics and amplitudes that occasionally caused a track relay to pick up momentarily while a train was passing over an IB. Interference of sufficient amplitude to pick up a track relay was not observed before the train reached this point, or after it was clear of this point, but only while it was over the point. Based on these observations and other supporting tests, it became clear that the interference in question is inductive in origin. Signals observed at NYCTA and BART were qualitatively similar to those seen at MARTA and CTA. The sources of the inductive interference are the inductive elements of the chopper propulsion system on the car.

Figure 5 shows the physical configuration of track, car, and IB that leads to generation of inductive interference. Pulsed magnetic flux from the "chopper box" containing the chopper control circuitry, typically mounted under the car, passes downward through the closed loops formed by the rails, car axles, and IB leads. The time-varying magnetic fluxes $\Phi_1(t)$ and $\Phi_2(t)$ produce emfs with polarities as shown:

$$\dot{\Phi}_{1,2}(t) = d\Phi_{1,2}(t)/dt = v_{1,2}(t) \qquad (1)$$

---

* T.C. Matty, R. Rhoton & W. Truman, Westinghouse Electric Corporation Transportation Systems Divsion, West Mifflin, PA., private communication.

GENERATION OF INDUCTIVE INTERFERENCE

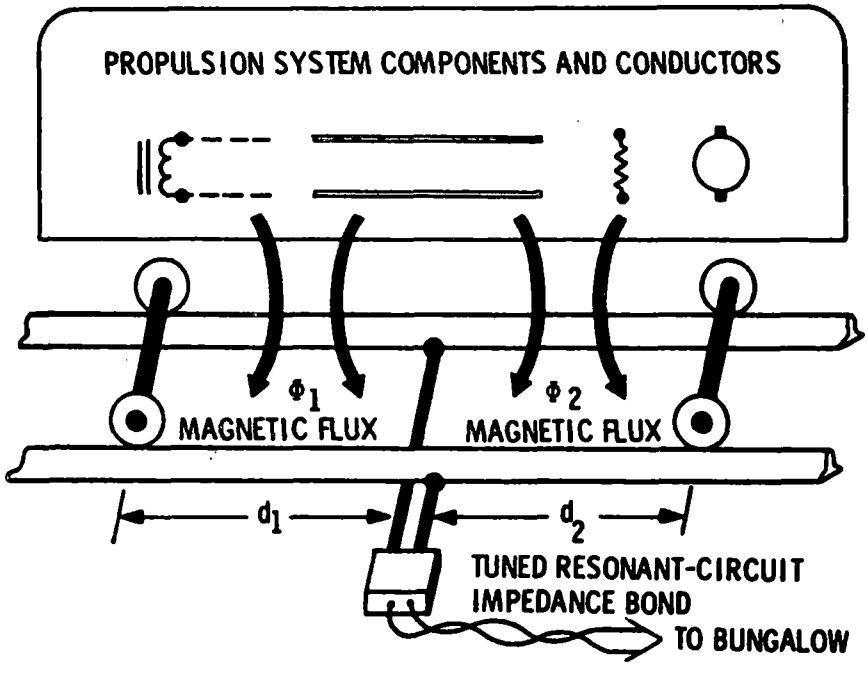

FIGURE 5. Configuration of car and signaling equipment leading to inductive chopper interference.

Figure 6 shows a simplified diagram of a typical rapid-transit chopper operating in the propulsion mode. (Different circuit connections, not shown, are used in regenerative braking modes.) Prior to gating on the main thyristor T_M, the commutation capacitor C_C is charged to the dc line voltage V_L, by transient current flowing through line filter reactor L_L, C_C, commutation reactor L_C, commutation diode D_C, motor smoothing reactor L_M, and the motor.

The main thyristor T_M is gated on to initiate a motor voltage pulse. Since the voltage across T_M then becomes zero, the commutation thyristor T_C then becomes forward-biased by amount V_L. Motor current through T_M, L_M, and the motor then rises. To turn off voltage applied to L_M and the motor, T_C is gated on, thus transferring the voltage across T_C to L_C. A commutation current pulse then starts in the clockwise direction through the closed loop formed by C_C, T_M, T_C, and L_C. This pulse is a sinusoid with frequency $f_c = 1/[2\pi\sqrt{(L_C C_C)}]$, typically appx. 10 times the chopper repetition frequency.

The commutation current pulse reverses polarity after the first quarter-cycle, and flows in the reverse direction through T_M, driving the total current through T_M to zero, allowing T_M to turn off. With T_M off, C_C once more charges as before.

The main producers of interference are the commutation reactor L_C and the motor smoothing reactor L_M. The spectral characteristics of interference produced by these components is dependent on their current waveforms. The commutation reactor has greatest potential for interference generation, since its peak current exceeds the motor current, and since its voltage and current waveforms are rapidly time-varying and rich in harmonics.

Figure 7 shows idealized waveforms of current through L_M and L_C, and the time derivative of resulting magnetic fluxes. The time derivative of L_M flux has a Fourier series expansion of the form

$$\dot{\Phi}_M(t) = \sum_{n=1}^{\infty} a_n \cos(2\pi n f_m t) \qquad (2)$$

where $$a_n = (2A/n\pi)\sin(n\pi\delta) \qquad (3)$$

and where f_m = chopper repetition frequency and δ = duty cycle.

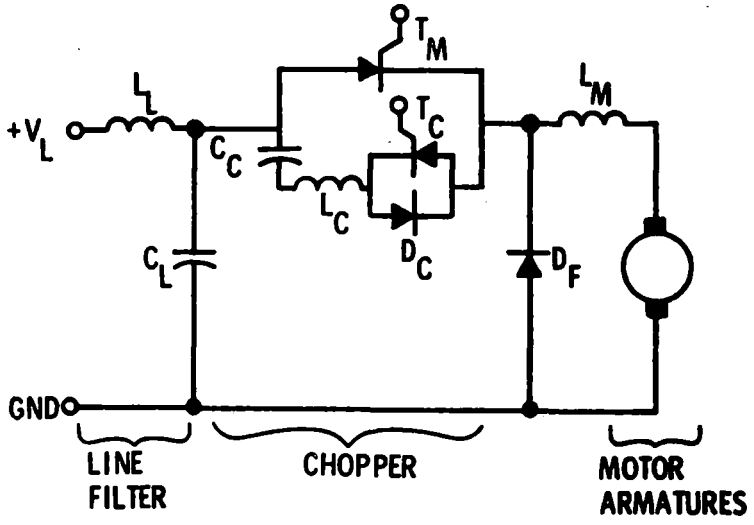

FIGURE 6. A chopper circuit showing wiring for propulsion mode. Power feed to $+V_L$ is from third rail or catenary, and ground return is to running rails.

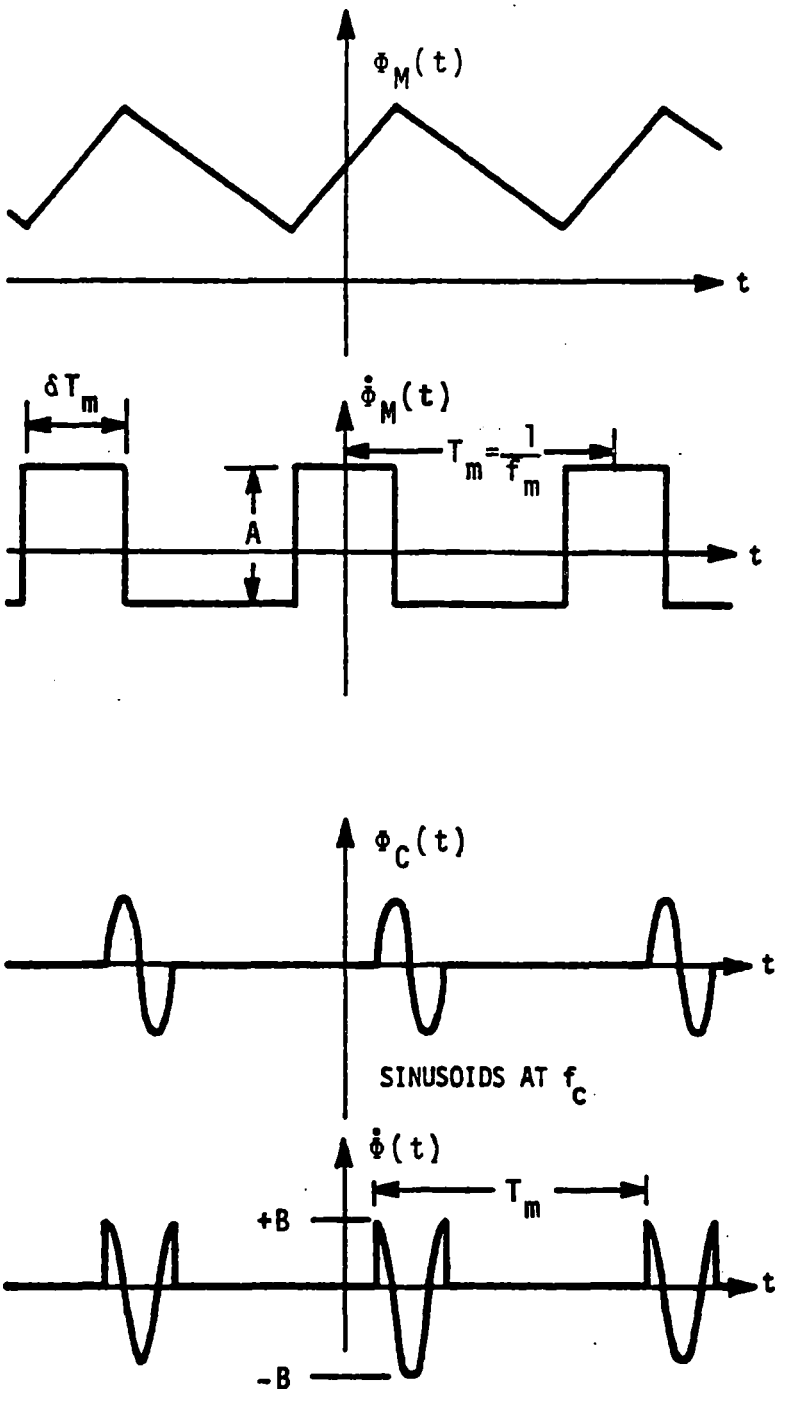

FIGURE 7. Idealized waveforms of motor smoothing reactor flux $\Phi_M(t)$, commutation reactor flux $\Phi_C(t)$, and corresponding emf's $\dot{\Phi}_M(t)$ and $\dot{\Phi}_C(t)$.

The derivative of commutation reactor flux has a Fourier series expansion of the form

$$\dot{\Phi}_C(t) = \sum_{n=1}^{\infty} b_n \cos(2\pi n f_m t - \theta_n) \qquad (4)$$

where

$$b_n = (-2B/\pi)\{nf_m^2/(f_c^2 - n^2 f_m^2)\}\sin(\pi n f_m/f_c), \quad \text{and}$$
$$\theta_n = n\pi\delta \qquad (5)$$

Figure 8 illustrates the fact that L_M and L_C jointly produce rich harmonic components of $\dot{\Phi}(t)$ for frequencies from f_m to well above f_c. Heinzerling & McElhenny have analyzed the spectra of inductive interference from choppers with different circuitry and consequently different current waveforms than discussed here, and have obtained qualitatively similar results [Ref. 16].

Other sources of magnetic flux are the other inductors in the circuit, electrical leads, braking resistors, and other power systems used for generating field currents (if separately excited motors are used) and auxiliary power. Often these other power systems are chopper-controlled. However, L_C and L_M of the propulsion system have been found to be the largest contributors to inductive chopper interference in most instances.

Equations (2) - (5) above indicate that inductive interference has an harmonic line spectrum characterized by individual components at discrete frequencies. This picture is complicated in practice by the fact that when a car starts from rest and motor back emf is small, very small duty cycles must be used to hold motor current to allowable values. Since minimum duty cycle with forced commutation is (f_m/f_c), some chopper systems control starting current by initially sweeping f_m upward from a low starting value to a normal operating value. Others control starting current by pulse skipping - leaving out a variable portion of motor current pulses in a pattern that is repetitive in the short term but variable in the long term. Either procedure complicates the spectrum.

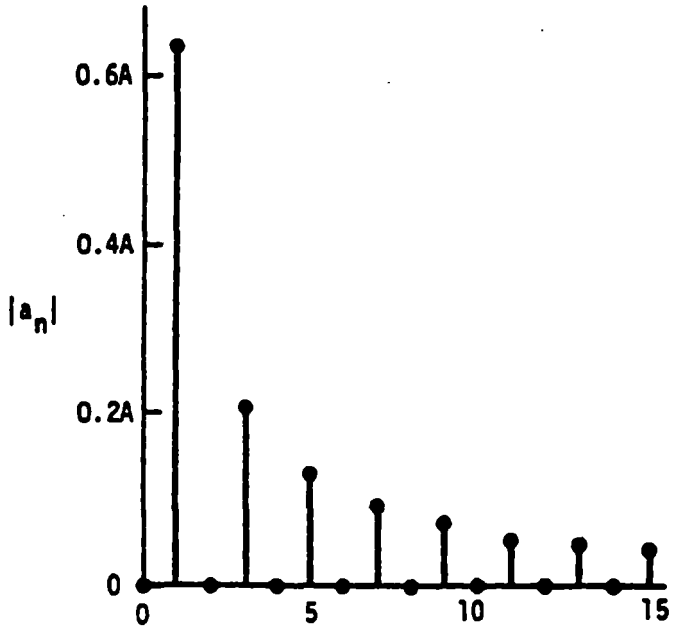

a) Fourier coefficients of $\dot{\Phi}_M$.

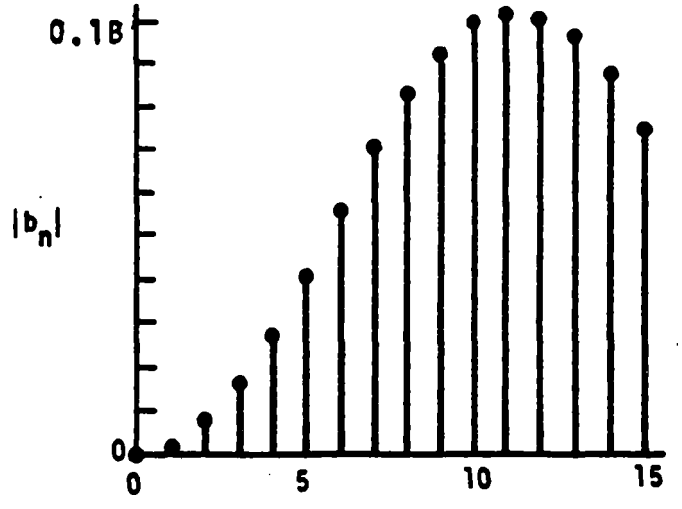

b) Fourier coefficients of $\dot{\Phi}_C$.

FIGURE 8. Amplitudes of Fourier series components of $\dot{\Phi}_M(t)$ and $\dot{\Phi}_C(t)$, for the case $f_c = 10\ f_m$ and $\delta = 0.5$.

All rapid transit choppers also control power by varying δ, thus influencing the relative strength of individual harmonics as illustrated by Eqn. (3). In addition, all harmonic components obviously vary in amplitude with the passage of a car past a fixed point.

Field observations indicate, however, that whereas the spectral characteristics of interference signals vary, they vary slowly compared to the receiver response time, which is the inverse of receiver filter bandwidth.

4. CHOPPER INTERFERENCE GENERATION: THE RAIL CIRCUIT

The rail-axle loops are characterized by their loop impedances $Z_{1,2}(d_{1,2},f)$. The impedance of the IB leads is noted by $Z_{b1}(f)$. The emfs, in conjunction with the impedances, yield the Thevenin equivalent source voltage and impedance, written in the frequency domain as

$$V_s(f) = (\dot{\Phi}_1 Z_2 - \dot{\Phi}_2 Z_1)/(Z_1 + Z_2) \tag{6}$$

$$Z_S = (Z_1 || Z_2) + Z_{b1} \tag{7}$$

The characteristics of Z_S can be estimated as follows: A pair of running rails of standard 143.5 cm (56.5") gauge has series loop impedance that above 1 kHz is practically all inductive (phase angle is greater than 80^0), with inductance of appx. 1.4 μH per meter of length. Thus, Z_S has the approximate behavior

$$Z_S(f) = jf[0.01 + 0.009 d_1 d_2/(d_1 + d_2)] \text{ ohms} \tag{8}$$

where d_1 and d_2 are in meters and f is in kHz.

The above relation neglects wheel-rail contact resistance, which is negligibly small when current is being conducted by the contacts. It also neglects rail-to-rail ballast shunting admittance, which is negligibly small for all except the dirtiest ballast conditions.

Figure 9 illustrates the resulting equivalent circuit relating car-generated magnetic flux to interference voltage into the IB. In spite of the fact that the transfer function

$$(V_{IB}/V_S) = Z_{IB}(f)/[Z_{IB}(f) + Z_S(f)] \tag{9}$$

is strongly frequency dependent, the effect of the relationship between Z_{IB} and Z_S on this transfer function is simplified in practice by the fact that frequency ranges of interest are very narrow ones that lie adjacent to where ZIB has its maximum values, typically between 0.15 and 0.5 ohms in magnitude

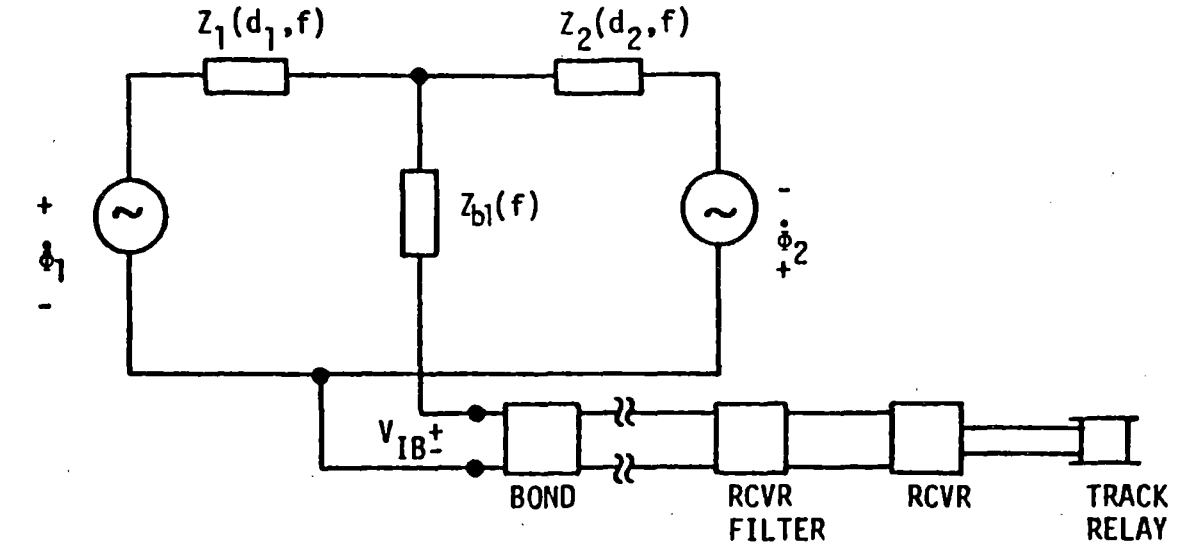

(a)

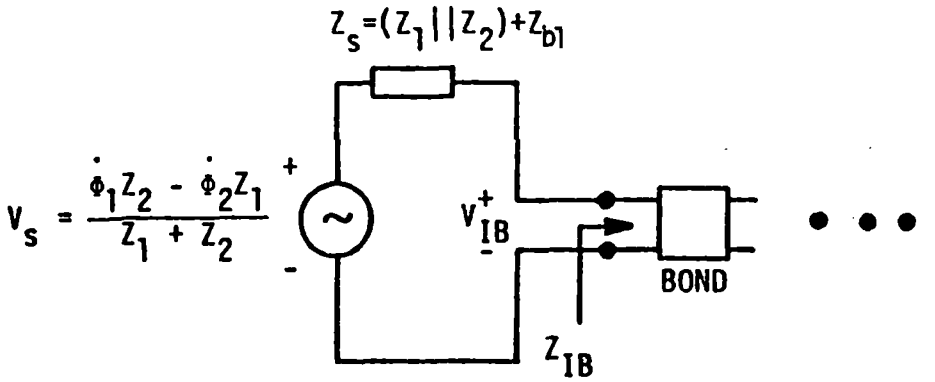

(b)

FIGURE 9. (a) Circuit for source of inductive interference; and, (b) its Thevenin equivalent.

(cf. Fig's 3, 4). Therefore, between 1 and 7 kHz, voltage division between Z_{IB} and Z_S attenuates V_S by an amount between 0 and 9 db at or near receiver frequencies.

The greater value above is illustrated by assuming that $d_1 = d_2 = 10$ m, f = 7 kHz, Z_S = j0.385 ohms from Eqn. (8), and Z_{IB} = 0.15 + j0 ohms. Then,

$$(V_{IB}/V_S)_{db} = 20 \log_{10}|[0.15/(0.15 + j0.385)]| = -9 \text{ db} \qquad (10)$$

A variety of factors influences the behavior of $V_S(t)$. The specific contributions of fluxes Φ_M and Φ_C to Φ_1 and Φ_2 depend upon the structure, placement, and orientation of components. Construction of the chopper box determines properties of eddy currents that can partially cancel the effects of currents in leads and components. The magnitude and phase relations of the various harmonic components of all flux sources depends on the mode of car operation. And finally, the variation of Φ_1, Φ_2, Z_1, and Z_2 with car position causes V_S to have a time-varying peak-to-peak amplitude, as is discussed in the following section.

5. OBSERVATION AND RECORDING OF CHOPPER INTERFERENCE SIGNALS

Examination of Figure 9 and Eqn. (9) shows that in the absence of a track circuit load, the Thevenin equivalent source voltage appears as the rail-to-rail voltage. This fact makes possible the observation and recording of V_S by use of instrumentation with sufficiently high input impedance. Knowledge of the frequency and time properties of V_S, coupled with behavior of Z_S, Z_{IB}, and other track circuit operating characteristics, then can be used to predict the response of track circuits to interference.

Figure 10 shows the instrumentation that has been used to observe and record V_S. The capacitor, resistor, and transformer protect the recording instruments from high-energy transients and imbalances due to propulsion currents in the rails. Tap changes on the transformer allow adjustment of signal level at recorder and spectrum analyzer input to match the dynamic ranges of these instruments. Lower cutoff frequency of the coupling circuit is 180 Hz - well below frequencies of interest.

The tape recorder meets IRIG Intermediate Band, Direct Record standards, and has record-playback response that is flat within 2 db from 70 Hz to 60 kHz when operated at 15 in/sec. The broad bandwidth allows capture of the transient characteristics as well as the frequency characteristics of signals.

The Fast Fourier Transform (FFT) spectrum analyzer has real-time response up to 20 kHz, but is typically employed in the 0-10 kHz mode. In this mode, it takes 1024 signal samples in each 40 msec sampling time window and calculates and displays the the magnitudes of the lowest 400 of 512 FFT components. Operation is called "real-time" since there are no time intervals between sampling time windows. The FFT analyzer's built-in Hann weighting function is used to suppress the spurious effects that otherwise arise when the sampling time window is not an integer multiple of signal periods long. [Ref. 18]

Sometimes the FFT analyzer is operated in the "MAX" mode, in which the maximum rms amplitude arising at each displayed frequency, for any sampling time window during a run, is stored and displayed. Such operation makes possible rapid determination of worst-case data across the spectrum. At other

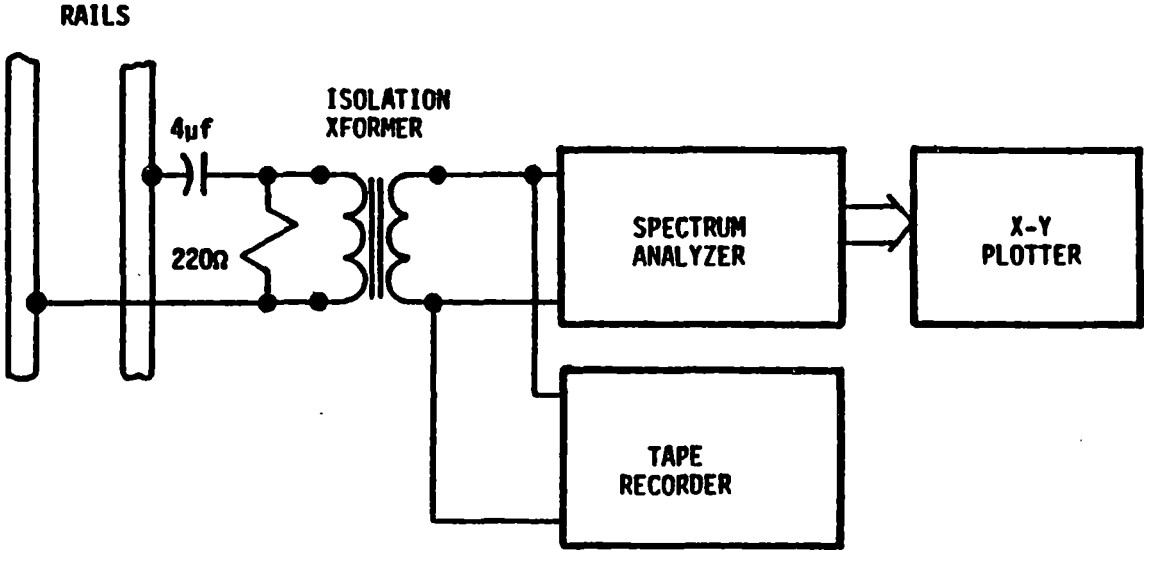

FIGURE 10. Instrumentation for observing and recording inductive interference.

times the analyzer is operated in the "E/1" mode, in which FFT spectra for signals in each sampling time window are consecutively calculated and displayed during the course of a run. This mode of operation allows direct observation of the time behavior of spectral characteristics.

Use of the tape recorder allows detailed analysis of interference signals in the laboratory. To assess validity of taped data, MAX-mode FFT spectra are recorded in the field by photos of the FFT analyzer's display or by means of an analyzer-driven X-Y plotter, and compared with similar spectra generated from tape in the lab. Amplitude calibration of the data gathering system is performed by injecting sine wave signals of known frequency and amplitude at the track terminals, measuring their amplitude at tape input, and playing them back in the lab.

MAX-mode spectra taken directly in the field and taken from tape in the lab typically agree within 2 db at any chopper harmonic frequency. Much useful information also is gained by simply listening to interference signals played through an audio amplifier and speaker, and by observing them in real time on an oscilloscope.

As a rail car passes the measuring point, the rail-to-rail voltage is observed to be a burst of pulses of complex and changing shape, that grows and decays in amplitude. The growth and decay can be explained by examination of Eqn. (6) and Figure 5: When d_1 is small, Φ_1 typically will be small, and Z_1 will be small, both of which cause V_S to be small. A similar situation occurs when d_2 is small. V_S will tend to be larger when d_1 and d_2 are nearly equal, provided the contributions to V_S from Φ_1 and Φ_2 are in phase.

Three snapshots of voltage waveform taken at successive times during the passage of a MARTA car past a measuring point are shown in Figure 11. In Fig. 11(a), the voltage pulse due to L_M is an upward-going square wave with a triangular portion added after the turnoff point. The pulse due to L_C is a downward-going cosine wave. Between (a) and (b), the L_M contribution inverts due to passage of L_M past the measuring point. Note that L_M was an air-core solenoid with vertical axis.. Between (b) and (c), the L_C contribution inverts when L_C, also a vertically-oriented air-core solenoid, passes the

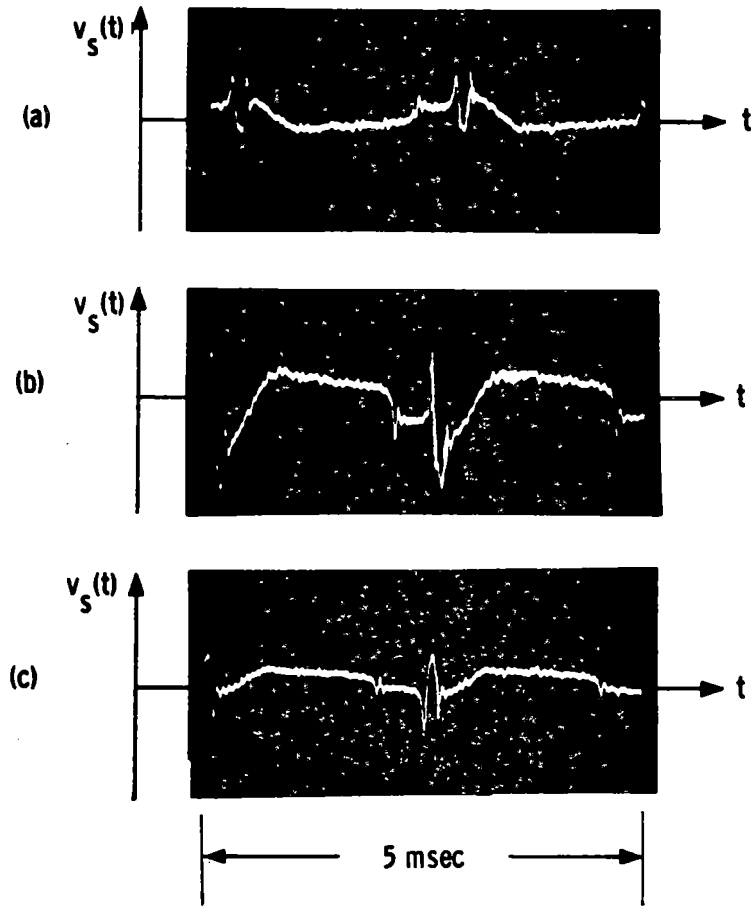

FIGURE 11. Waveforms of open-circuit rail-to-rail voltage during passage of a car.

measuring point. Duty cycle is small but increasing slightly in these photos, since the car was accelerating from rest.

Figure 12 shows an FFT spectrum calculated from one 40 msec sampling window during the passage of the above car (lower curve), and the MAX-mode spectral display resulting from the passage of the entire four-car train (upper broken curve). It is apparent that individual spectral lines change amplitude as the train passes, and spectral shape changes as well. To avoid smearing of the MAX-mode display by frequency sweeping, the spectrum analyzer was started after f_m had reached its final value of 400 Hz.

Time variation of individual spectral lines can be observed by playing interfering signals through a narrow-band filter that passes one line, and observing the amplitude of its envelope as a function of time. The ninth chopper harmonic for the above run was selectively observed by use of a filter with 100 Hz bandwidth and 3600 Hz center frequency. A standard frequency-domain spectrum analyzer operated in the unswept mode served as filter and detector.

The behavior of rms amplitude vs. time is shown in Figure 13. Passage of each car causes a burst of signal. The amplitude of each burst is scalloped by changing duty cycle. Note that as the last car in the train got to the measuring point, the train reached the speed at which 100% duty cycle can be used, and the choppers stopped chopping.

Figure 12 shows amplitude levels that are significantly greater than receiver thresholds throughout the 1-7 kHz range. In fact, during operation of MARTA trains over track circuits while the above data were being taken, momentary lifting of track relays was observed in those locations in which chopper harmonics fell within receiver filter passbands.

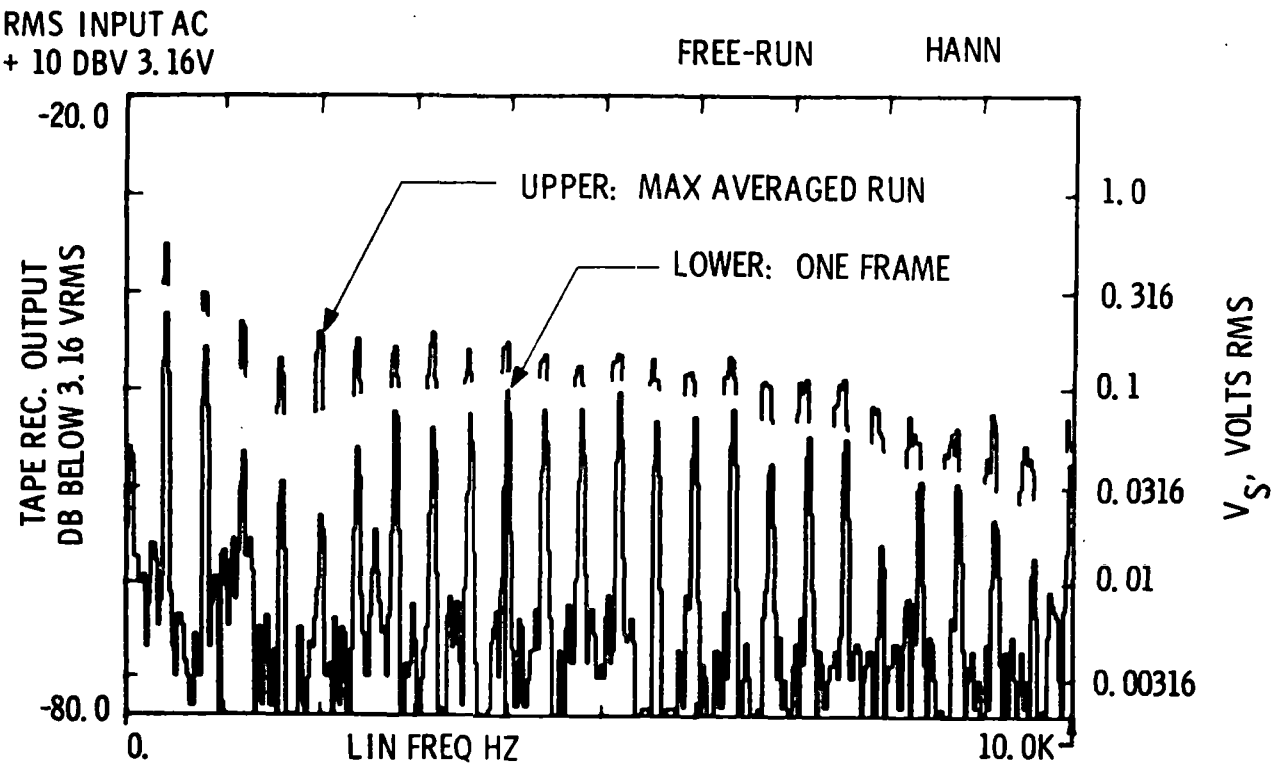

FIGURE 12. FFT spectral plots of rail-to-rail inductive interference voltage. Left-hand scale gives signal amplitude played back out of tape recorder. Right-hand scale gives rail voltage into tape recorder.

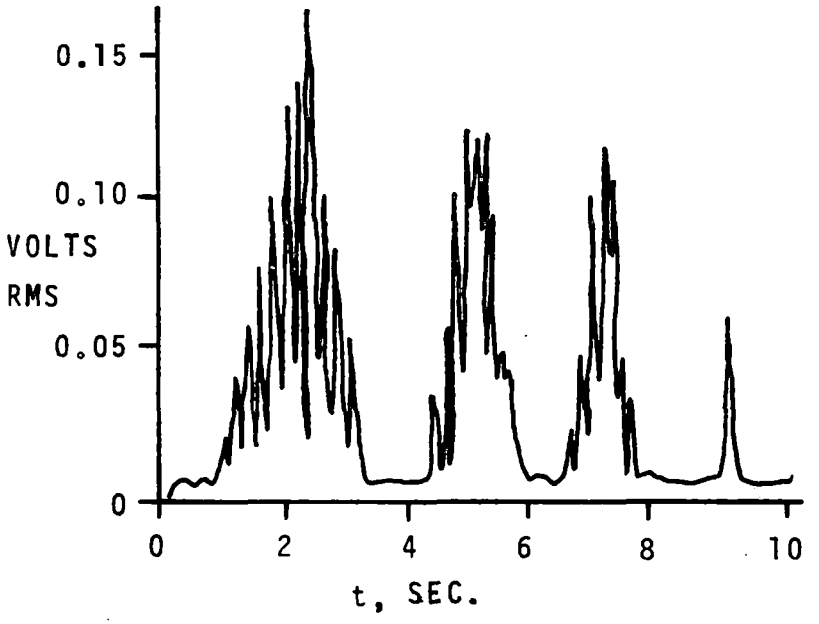

FIGURE 13. RMS amplitude of a single interference spectral line vs. time as a train passes. Line shown is 9th harmonic at 3600 Hz.

6. DIAGNOSIS AND REDUCTION OF CHOPPER INTERFERENCE

Manufacturers of chopper-controlled propulsion systems ("chopper manufacturers") have employed a variety of techniques to estimate anticipated levels and diagnose sources of chopper interference while chopper systems are still in development and before they are mounted on cars. The primary one was developed by Rudich [Ref. 11], who used aluminum tubes of 1.5-2.0 cm dia. to simulate car axles and aluminum tubes of 2.5-9.4 cm dia. to simulate running rails. The tubes were securely fastened together to form a closed rectangular loop whose width was the standard rail gauge and whose length was the interior car wheelbase. The loop was positioned over or under the chopper box in the lab in a manner that duplicated actual geometry as depicted in Figure 5. Such an arrangement accurately models $Z_S(f)$ and $V_S(f)$ as a function of d_1 and d_2.

Matty, Rhoton, and Truman (see footnote, pg. 11) have found that the loop can be made shorter than the car wheelbase, provided the loop is long enough to capture most of the magnetic flux emanating from the chopper box, and provided additional compensating inductance is added to the axle tubes.

Use of the above technique allows the chopper manufacturer to observe in the lab the effects on interference levels of changes in component structure and positioning, lead dress, and chopper box construction. Effects of spectral characteristics due to sweeping chopper frequency, pulse skipping, and varying duty cycle can also be observed.

Chopper manufacturers have reduced the levels of stray magnetic flux and the inductive coupling of chopper components with the rail loop under the car. Methods they have used include choosing inductor designs that produce less stray flux, orienting inductors so that less net stray flux passes downward through the rail loop, paying strict attention to lead dress and cabling, and controlling operating cycles to avoid generation of harmonics between normal chopper harmonic lines.

Efforts have been undertaken to simulate chopper interference effects on signaling circuits. Vaughn has developed a microprocessor-based system for synthesizing chopper interference waveforms with known characteristics [Ref.

13]. This system allows the signal manufacturer to examine the susceptibility of track circuit receivers to interference signals with specific characteristics.

Ideally, it would be desirable to amplify recorded or simulated signals corresponding to V_S and play them directly into the track terminals of track circuits at signal levels corresponding to the worst that would be expected. However, the large peak amplitude of interference impulses contributed by the commutation reactor, coupled with the low magnitude of Z_S and Z_{IB} at most frequencies, leads to very high levels of instantaneous current that an amplifier must supply to the IB input leads. One commercially available op-amp type power amplifier having a peak current rating of 5 amperes has been used for this purpose at reduced voltage levels. Signals recorded in the field or lab can be amplified and fed to track receiver filter inputs where impedance levels are higher.

The most complete and realistic simulation of chopper interference is one that involves the cooperative efforts of chopper and signal manufacturers, in which actual signal equipment is hooked to the rectangular loop simulating track and axles.

While chopper manufacturers have been investigating use of new components that generate less stray flux, and component orientations and circuit layouts that yield less net contribution to Φ_1 and Φ_2, signal manufacturers have been developing new track circuit designs that are more tolerant of interference.

One such design employs transmission of independently coded signals for train control and track circuit operation [Ref. 11]. The train control signal is of variable code rate and carrier frequency, and is received and decoded on board the train in normal fashion. The track circuit signal is of fixed carrier frequency and fixed code rate of appx. 1 Hz. Following envelope detection of the track circuit signal at the track circuit receiver, a fixed-tuned second detector with bandwidth of appx. 1 Hz then is employed to discriminate between true and interference signals. This type of receiver will only respond to repetitive signals whose repetition rate is very near that of true signals. Since in this scheme the track circuit transmitter

transmits the instantaneous sum of train and track signals instead of transmitting them in interleaved bursts, the track circuit transmitter must be capable of generating approximately twice the previous peak output voltage.

Another design employs transmission of train signals and track signals in interleaved bursts as discussed in Sec. 2. In this scheme, the track receiver produces an envelope-detector output whose frequency is the code rate. This waveform then goes to a synchronous second detector, whose reference signal is the original code rate modulation waveform from the transmitter [Ref's 12, 13].

Both of the improved track signal detection techniques described above provide a much smaller effective receiver bandwidth than that provided by the broadband asynchronous technique previously used. In either new technique, the noise bandwidth of the receiver is that of the second detector rather than that of the receiver filter - on the order of 1 Hz rather than 100 Hz.

It should be noted that the use of these frequency-domain coding techniques to achieve compatible operation of choppers and audio-frequency track circuits was preceded by the BART signaling system, in which digitally encoded and decoded FSK track signals are used to mitigate the effects of interference [Ref. 17].

7. CONCLUSION

Since its original observation, the effects of inductive chopper interference on audio-frequency track circuits have become well understood. Knowledge of the inductive coupling mechanism and behavior of the circuit composed of car, rails, and track circuitry paved the way for mitigation of chopper interference.

The cooperative activities of signal and propulsion manufacturers, transit authorities, and other investigators have made possible the timely correlation of laboratory and field data, and have paved the way for solution of the problem of inductive chopper interference. Specific modifications to older techniques of propulsion system design and signaling system design have been developed, and these modifications have resulted in compatible operation of chopper-controlled propulsion systems and audio-frequency signaling systems.

Diagnostic techniques have been developed whose use will mitigate the problems of inductive interference in future rapid transit systems [Ref. 10].

REFERENCES

1. V.D. Nene, "The status of advanced propulsion systems for urban rail vehicles," MITRE Technical Report No. MTR-79W00022, Metrek Div., MITRE Corporation, McLean, VA 22102, Feb. 1979. Chapter 3 - Chopper controlled propulsion equipment. (Report contains an extensive list of references.)

2. "Automatic train control in rail rapid transit," U.S. Congress Office of Technology Assessment, May 1976. Chapter 3 - Automatic train control. Appendix B - Automatic train control technology.

3. P. Chowdhuri & D.F. Williamson, "Electrical interference from thyristor-controlled dc propulsion system of a transit car," IEEE Transactions on Industrial Applications, Vol. IA-13, pp. 539-550, 1977.

4. B. Mellitt, "Signal interference effects with chopper controlled traction," Railway Gazette International, Nov. 1979, pp. 999-1003.

5. F.R. Holmstrom, "The model of conductive interference in rapid transit signaling systems," Proceedings of the IEEE Industrial Applications Society 1985 Annual Conference, Toronto, 6-11 Oct. 1985. To be published in the IEEE Transactions on Industrial Applications.

6. F.R. Holmstrom, "Conductive interference in rapid transit signaling systems. Volume I: Theory and data," U.S. Dept. of Transportation Report No. UMTA-MA-06-0153-85-5, U.S. Dept. of Transportation, Transportation Systems Center, Cambridge, MA 02142.

7. L.A. Frasco, R. Gagnon, and F.R. Holmstrom, "Electromagnetic compatibility of advanced propulsion systems," Proceedings of the International Conference on Advanced Propulsion Systems for Urban Rail Vehicles, sponsored by UMTA/DOT, Washington, DC, Feb. 1980, pp. 193-213.

8. L.A. Frasco, R. Gagnon, & F.R. Holmstrom, "Choppers affect operation of AF track circuits," Railway Gazette International, April 1980.

9. L.A. Frasco, "Rail transit vehicle EMC testing," Proceedings of the Federal Railroad Administration EMC Symposium, Pueblo, CO, 13-15 May 1980.

10. "Inductive interference in rapid transit signaling systems - Volume II: Suggested test procedures," DOT Report No. UMTA-MA-06-0153-85-8, Urban Mass Transportation Administration, U.S. Dept. of Transportation, to be published, 1986. Preliminary form of this document was, "Recommended practices for rail transit intra-system electromagnetic compatibility of vehicular electrical power and track circuit signaling subsystems - Volume 1: Inductive recommended practices," U.S. Dept. of Transportation, Urban Mass Transportation Administration, Report No. DOT-TSC-UM204-PM-82-21,I, May 1982.

11. J. Hoelscher & R. Rudich, "Compatibility of rate-coded audio frequency track circuits with chopper propulsion drive in transit systems," Proceedings of the International Conference on Railways in the Electronic Age, sponsored by the I.E.E., London, England, 17-20 Nov. 1981, pp. 128-135.

12. D.E. Stark, "Signaling system evolution: Meeting the challenge of electromagnetic compatibility in modern rail transit systems," presented at the joint meeting of the APTA Technical Liaison board and Rail Transit EMI/EMC Technical Working Group, DOT/TSC, Cambridge, MA 02142, 25-26 Jan. 1984.

13. T.C. Vaughn, C. Mokkapati & R.P. Bozio, "Electromagnetic interference mitigation of audio frequency signaling system for Baltimore Region Rapid Transit System," U.S. Dept. of Transportation Report No. UMTA-MD-06-0072-83-1, Nov. 1983. Prepared by Union Switch & Signal Division, American Standard, Inc., Pittsburgh, PA.

14. C. Weinstein & J. Healey, "MARTA propulsion system," Proceedings of the International Conference on Advanced Propulsion Systems for Urban Rail Vehicles, sponsored by UMTA/DOT, Washington, D.C., Feb. 1980, pp. 26-42.

15. D.R. Phelps, "Testing of the G.E. chopper propulsion system at NYCTA," presented at the American Public Transit Association Rapid Transit Conference, 19 June 1980.

16. E.W. Heinzerling & S.W. McElhenny, "The compatibility of thyristor propulsion and rate-coded audio-frequency track circuits," Proceedings of the IEEE Industrial Applications Society 1980 Annual Conference, Cincinnati, October 1980.

17. G.D. Friedlander, "BART's hardware - from bolts to computers," IEEE Spectrum, Vol. 9, No. 10, Oct. 1972, pp 60-72.

18. O.E. Brigham, The Fast Fourier Transform, Prentice Hall, Engelwood Cliffs, NJ, 1974.

100 copies

U.S. Department
of Transportation

**Research and
Special Programs
Administration**

Kendall Square
Cambridge, Massachusetts 02142

Postage and Fees Paid
Research and Special
Programs Administration
DOT 513